

Original Article

# Optimization study of CO<sub>2</sub> inerting parameters in goaf based on coal sample oxidation characteristics

Shuoran Huang<sup>a,b,\*</sup>, Zongxiang Li<sup>a,b</sup>, Yu Liu<sup>a,b</sup>, Ji Wu<sup>a,b</sup>

<sup>a</sup>College of Safety Science and Engineering, Liaoning Technical University, Fuxin, Liaoning 123000, China

<sup>b</sup>Key Laboratory of Mine Thermodynamic Disaster & Control of Ministry of Education, Huludao, Liaoning 125105, China

## ARTICLE INFO

### Keywords:

CO<sub>2</sub> inerting parameters  
Oxidation characteristics  
Sealed coal oxidation experiment  
Spontaneous combustion "three zones"

## ABSTRACT

The spontaneous combustion of residual coal in Goaf seriously threatens the safety of coal mining. Injecting CO<sub>2</sub> into goaf can prevent the spontaneous combustion of residual coal and store CO<sub>2</sub>. The suffocated (steady state) oxygen concentration of coal samples is a key indicator for evaluating the effectiveness of CO<sub>2</sub> inertization. To enhance the accuracy of the CO<sub>2</sub> injection parameter design, the suffocated oxygen concentration of the Jiudaoling (JDL) coal samples was determined through sealed oxidation experiments. Combined with field measurements and numerical simulations, a numerical model of the Goaf was established, and the suffocated oxygen concentration was applied to the study of CO<sub>2</sub> inerting characteristics in the (Jiudongling) JDL coal mine. The study results demonstrate a positive correlation between the degree of coal metamorphism and the suffocated oxygen concentration. With the gas injection port moving away from the working face, the maximum extent of the oxidation zone initially decreased and then increased. The relationship between the CO<sub>2</sub> injection rate and width of the spontaneous oxidation zone is inversely exponential. The optimal injection location was determined to be 43 m from the working face on the intake air side, with an optimal injection rate of 156.9 m<sup>3</sup>/h.

## 1. Introduction

Currently, approximately 95% of coal extraction in China occurs underground [1]. In key coal mines across the country, the proportion of mines severely affected by coal spontaneous combustion (CSC) is as high as 56% [2]. Due to the ongoing reduction of surface coal reserves, coal mining is transitioning into the phase of deep extraction. The increase in coal mining depth leads to higher coal seam gas content and mining temperatures, which in turn amplifies the propensity for CSC [3], a phenomenon frequently observed in Goaf. Due to its slow-burning process and lack of visible flames, the fire source is difficult to locate, resulting in prolonged burning [4,5]. Additionally, CSC in mines results in the production of substantial toxic gases, which not only disrupts the efficient operation of the mine ventilation system but also may lead to toxic gas accumulation and explosions, thereby posing a significant risk to miners' safety [6-8]. Therefore, effectively preventing and controlling the occurrence of CSC in Goaf is of utmost importance.

Identifying the "three zones" of spontaneous combustion within Goaf establishes a foundational theory for the prevention and control of CSC. The determination of the "three zones" of spontaneous combustion in goaf mainly utilizes three approaches, centered on the measurement of wind velocity through leaks, O<sub>2</sub> concentration, and the rate of temperature increase, with the approach based on O<sub>2</sub> concentration being commonly applied in engineering practice [9-11]. Xu *et al.* [12] carried out a theoretical, quantitative study of the delineation of the "three zones" in Goaf, proposed the concept of minimum safe advance speed, and provided a calculation method. Xie *et al.* [13] conducted an examination of the distribution condition of floating coal in goaf

and proposed a theory that spontaneous combustion "three zones" are present in both the longitudinal direction and the vertical extent of the goaf and mining face. Building on this, they further introduced the concept of spatial spontaneous combustion "three zones" and considered key indicators such as O<sub>2</sub> concentration and floating coal thickness in the delineation process. Song *et al.* [14] proposed criteria for delineating the spontaneous combustion "three zones" in high-gas goaf areas, considering the dilution and oxidation consumption of methane in goaf. Wei *et al.* [15] used O<sub>2</sub> concentration as a standard to delineate the spontaneous combustion "three zones" within the Goaf and found that the "Y" ventilation system, in contrast to the "U" system, led to an expansion in both the depth and breadth of the cooling and oxidation zones within the goaf. Gui *et al.* [16] explored the effects of the airflow ratio between the conveyor alley and the return airway on the distribution of the spontaneous combustion "three zones" within the goaf. The study found that an increase in the airflow ratio led to a proportional expansion of the oxidation zone's width within the goaf, while the impact on the cooling zone was relatively minor. The delineation of spontaneous combustion "three zones" within a goaf typically employs an O<sub>2</sub> volume fraction of 8% or 10% to serve as the demarcation standard between the oxidation zone and the suffocation zone [17]. However, this generalized approach does not fully consider the actual production conditions of coal samples, nor does it provide a sufficiently accurate basis for the precise assessment of spontaneous combustion risks in specific coal mine goaf areas [18].

Injecting inert gases such as N<sub>2</sub> and CO<sub>2</sub> into the goaf is a crucial strategy for the management and suppression of CSC within the goaf. The CO<sub>2</sub> fire prevention and extinguishing technology, due to its

### \*Corresponding author:

E-mail address: 2570602309@qq.com (S. Huang)

Received: 31 December, 2024 Accepted: 20 February, 2025 Epub Ahead of Print: 31 March 2025 Published: \*\*\*

DOI: 10.25259/AJC\_337\_2024

heavy gas sinking properties, offers advantages such as high inerting efficiency, good explosion suppression performance, and low cost, and has gradually gained attention and widespread application in the field of goaf fire prevention and extinguishing [19,20]. Due to the particularity of goaf, it is difficult for personnel to safely enter the area [21]. Hence, Computational Fluid Dynamic (CFD) tools are extensively utilized within the domain of goaf inerting technology [22]. Hao *et al.* [23] studied the influence of CO<sub>2</sub> injection location on the temperature of high-temperature spots within the oxidation zone of the goaf. Their findings indicate that as the CO<sub>2</sub> injection location moves progressively further from the working face, the temperature at the high-temperature spots in goaf initially drops rapidly and then gradually increases, exhibiting a linear growth pattern. Huang *et al.* [24] found that the absence of overlap between the inerted zone and the spontaneous combustion hazard zone is the fundamental reason for the low effectiveness of inerting. Consequently, they adjusted the inerting parameters to reduce the diffusion of inert gas into non-target areas. Qiao *et al.* [25] compared the oxidation zone areas after injecting N<sub>2</sub>, boiler gas, and CO<sub>2</sub> into the goaf and found that the oxidation zone area was smallest when CO<sub>2</sub> was injected. Additionally, they determined the critical injection rate of CO<sub>2</sub> to be 1750 m<sup>3</sup>/h. The width of the oxidation zone is a core indicator for evaluating the effectiveness of inerting. However, research on determining the extent of the oxidation zone based on the oxidation characteristics of coal seams and optimizing the gas injection parameters in goaf remains relatively scarce.

Therefore, in this study, a sealed coal oxidation experiment was utilized to ascertain the oxidative traits of coal specimens. Consequently, the spontaneous combustion “three zones” were precisely delineated, and the experimental results served as the basis for numerical simulation. By combining numerical simulations with field measurements, a three-dimensional model of the goaf was established to study the effects of injection port location and injection rate on the CO<sub>2</sub> inerting effectiveness in goaf. The optimal injection port location and injection rate were ultimately determined, which established a theoretical foundation for the optimization of CO<sub>2</sub> fire prevention and extinguishing techniques in goaf.

## 2. Materials and Methods

### 2.1. Sealed coal oxidation experiment

The process of CSC is typically categorized into three distinct phases: the initial incubation phase, the subsequent self-heating phase, and the final burning phase [26]. The initial incubation period is a critical stage for preventing CSC and monitoring coal mine fires [27]. To obtain the steady state oxygen concentration of coal samples during the initial incubation period under continuously varying oxygen concentrations, which was used as the criterion for dividing the oxygen concentration of the suffocation zone in the simulation, this study employed a sealed oxidation experiment.

#### 2.1.1. Coal sample preparation

The study involved three coal samples with different degrees of metamorphism, collected from JDL (Jiudaoling), DW (Duanwang), and DY (Dayan) mines. The block coal samples, sourced from the coal mining face, were sealed and then conveyed to the laboratory. There, they were crushed using a crusher and subsequently sieved to produce small coal samples with a particle size of 0 to 2 mm for experimental use. The process of preparing the coal samples has been shown in Figure 1.

#### 2.1.2. Experimental apparatus

The experimental apparatus includes a coal sample can, a constant temperature chamber, a gas flowmeter, a gas concentration sensor chamber, an air pump, a preheat tube, a thermocouple, and a computer. The experimental setup is shown in Figure 2. The coal sample can is a metal can with certain thermal insulation properties. The can is placed in a constant temperature chamber, with the temperature set at 30°C. The gas concentration sensor chamber contains an electrochemical O<sub>2</sub> sensor, which is utilized for tracking the O<sub>2</sub> concentration within the sealed experimental circuit. The O<sub>2</sub> sensor has a range of 0-25%. The air pump is a diaphragm circulation pump with good sealing

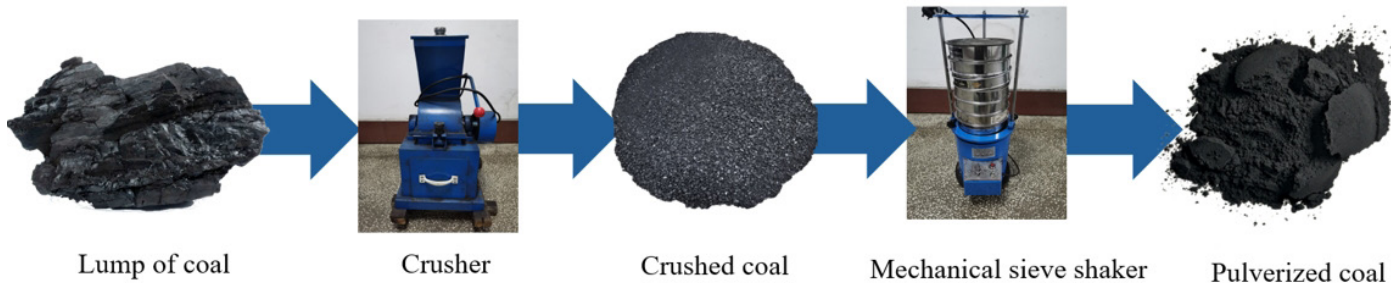


Figure 1. Coal sample preparation process.

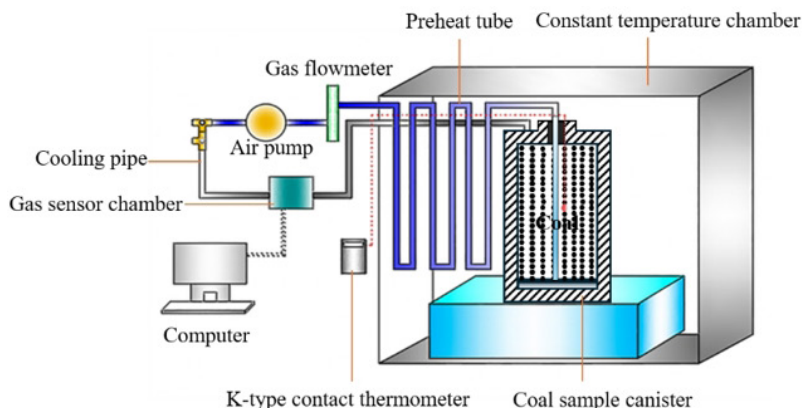


Figure 2. Sealed oxidation experimental apparatus.



properties. The temperature measurement device employed is a K-type thermocouple, which serves to track the temperature fluctuations within the coal specimen. The coal sample was preheated to the experimental temperature, the air pump was activated, and the gas flowmeter was adjusted to open the closed circuit, allowing a large volume of air to be rapidly injected into the pipeline. Once the  $O_2$  concentration within the experimental setup matched the ambient air concentration, the experimental pipeline was resealed to conduct the sealed oxidation experiment, and the changes in  $O_2$  concentration during the experiment were recorded.

### 2.1.3. Calculation principle of the sealed oxidation experiment

In a sealed environment, the total amount of gas in the experimental pipeline and coal sample remains unchanged. During the incubation phase of CSC, the sample experiences gradual oxidation, leading to a persistent decline in the  $O_2$  concentration within the gas and eventually reaching a steady state.

The  $O_2$  concentration  $c(\tau)$  is approximately in accordance with a negatively exponential distribution, as shown in Eq. (1) [28]:

$$c(\tau) = C_b + (C_0 - C_b) \cdot e^{-\lambda_c \tau} \quad (1)$$

where  $C_b$  is the steady state value of the  $O_2$  concentration, %.  $C_0$  is the original  $O_2$  concentration, %.  $\lambda_c$  is the  $O_2$  concentration decay rate,  $\text{min}^{-1}$ .  $\tau$  is the time, min.

When the  $O_2$  concentration is  $C_\phi$ , the volume  $O_2$  depletion rate within the coal specimen vessel, as shown in Eq. (2) [29].

$$\gamma = -0.4464\lambda_c(c_0 - c_\phi) \quad (2)$$

where,  $\gamma$  is the volume  $O_2$  depletion rate when the  $O_2$  concentration is  $C_\phi$ ,  $\text{mol}/(\text{m}^3 \text{min})$ .

## 2.2. On-site testing

In order to clearly define the extent of the spontaneous combustion “three zones” in the goaf of the JDL coal mine and to provide the necessary support for the  $CO_2$  injection simulation within the goaf. The  $O_2$  concentration within the goaf was tracked using tubes that were embedded in advance, capturing the variations in  $O_2$  concentration as the mining face progressed. The positions of the sampling pipelines have been shown in Figure 3, where they are installed in both the intake and return airways. The set of tubes located on the intake airway is marked as 1#, while the set of tubes on the return airway is marked as 2#.

## 2.3. Numerical simulation

ANSYS FLUENT is one of the advanced commercial Computational Fluid Dynamics (CFD) software packages. Using this software, a CFD model was established, and the distribution of oxygen concentration in goaf was simulated under different gas injection parameters.

### 2.3.1. Model construction

According to the circumstances pertaining to the E1S6 mining face within the JDL coal mine, a physical model of the goaf was constructed,

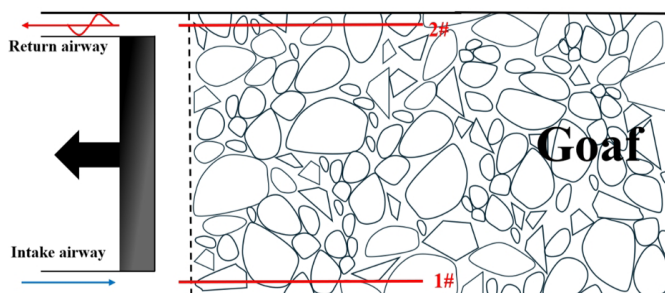


Figure 3. Tube bundle layout diagram.

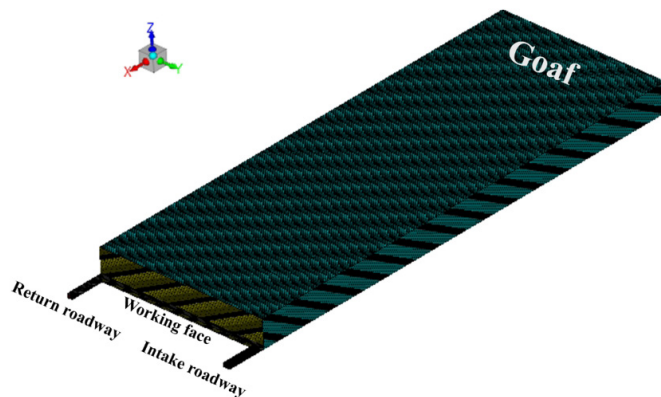


Figure 4. Goaf model.

as has been illustrated in Figure 4. The modeling origin point (0, 0, 0) is located at the bottom intersection of the return airway working face and the goaf. The dimensions of the goaf are  $400 \text{ m} \times 150 \text{ m} \times 25 \text{ m}$  (length  $\times$  width  $\times$  height), the intake airway is  $30 \text{ m} \times 4.5 \text{ m} \times 3 \text{ m}$ , and the return airway is  $30 \text{ m} \times 5.83 \text{ m} \times 3 \text{ m}$ . The scale ratio of the model size to the real size was 1:1.

### 2.3.2. Parameter settings

In this model, the boundary at the inlet is defined as a ‘velocity-inlet.’ The entrance of the intake airway at the working face is defined as ‘inlet1,’ while the injection point is identified as ‘inlet2,’ and the terminus of the return airway is designated as ‘outflow.’ The boundaries at the junction of the working face with the goaf, along with those between the working face and the intake and return airways, are designated as ‘interface.’ All external boundaries, excluding the intake and return airways, are established as ‘walls.’ The Re-Normalisation Group (RNG)  $k-\epsilon$  modeling approach is utilized, with Gambit automatically setting the complete three-dimensional domain as a fluid region. The goaf is a heterogeneous porous medium, and the RNG  $k-\epsilon$  turbulence model can effectively handle complex flows with high strain rates and large streamline curvatures [30]. It can also adjust turbulence parameters according to the characteristics of the porous medium, thereby adapting to the complex medium environment. Considering that the fluid flow within the goaf is turbulent at low Reynolds numbers, the Differential Viscosity Model is chosen. The goaf is meshed with hexahedral elements, with a mesh size of 0.5 m. The injection ports are set within a range of 20 to 60 m along the intake airway of the working face, with a total of five injection ports. The interval between each injection port is 10 m, and the  $CO_2$  concentration at the injection ports is set to 100%. The parameter settings are shown in Table 1.

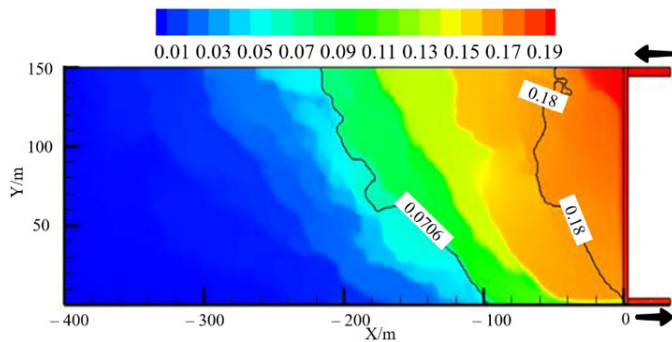
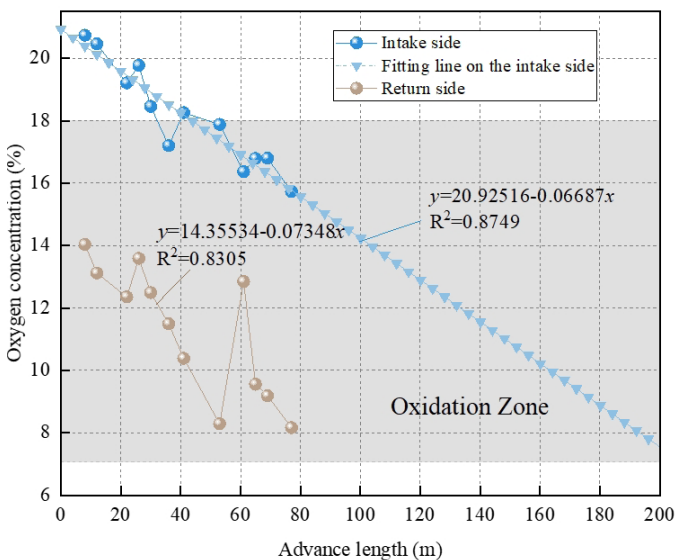
### 2.3.3. Model reliability

Figure 5 illustrates the  $O_2$  concentration distribution within the goaf when no additional  $CO_2$  has been injected. Based on the steady-state  $O_2$  concentration obtained from experiments, the simulation results were analyzed, delineating the intake side of the goaf into a 48 m cooling zone, a 167 m oxidation zone, and a 185 m suffocation zone. For the return side, the oxidation zone is 98 m wide, and the suffocation zone stretches to 302 m. The relationship between the actual measured  $O_2$  concentration values within the goaf and the distance from the working face has been depicted in Figure 6. According to the fitting results, the dimensions of the oxidation zone span approximately 163 m on the intake side of the goaf, while on the return side, they are around 99 m. Comparison with numerical simulation results demonstrates that the error in the intake side’s oxidation zone extent is 2.3%, and on the return side is 1.02%, thereby confirming that the computational outcomes of the constructed model have a high degree of reliability.

**Table 1.** Physical model parameters.

Category	Simulation condition
Inlet boundary condition	Velocity-inlet
Outlet boundary condition	Outflow
Goaf	400 m×150 m×25 m; RNG <i>k-ε</i> , Differential Viscosity Model
Working face	150 m×4.0 m×2.8 m
Return airway	30 m×4.5 m×3m
Intake airway	30 m×5.83 m×3m

RNG: Re-normalisation group

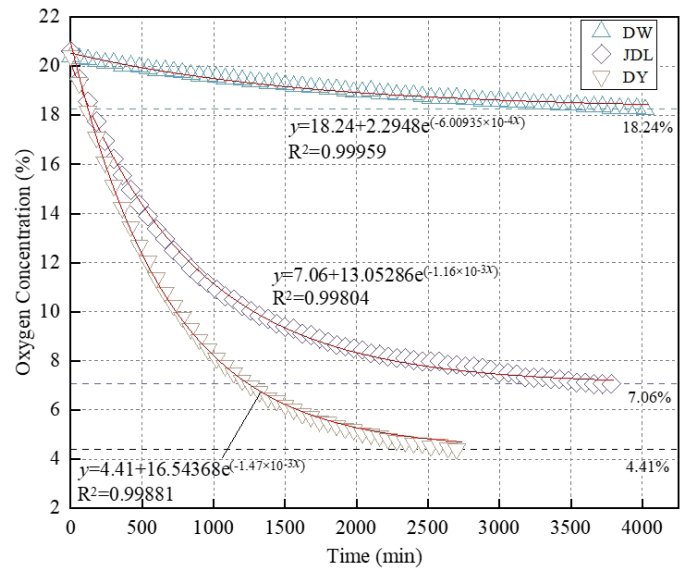
**Figure 5.** Initial O<sub>2</sub> concentration distribution.**Figure 6.** Curve of measured O<sub>2</sub> concentration versus distance from the working face in the goaf.

### 3. Results and Discussion

#### 3.1. Suffocated (steady state) oxygen volume fraction

As the oxidation reaction of the coal sample continues, the oxygen concentration gradually decreases and eventually reaches a stable oxygen concentration. Figure 7 illustrates the trend line correlating the oxygen concentration from the sealed oxidation experiment with elapsed time.

Coal is a complex macromolecular organic substance. During the coal formation process, a range of elements, including geological actions and storage conditions, exert influence, resulting in different degrees of metamorphism. With the escalation of metamorphic grade in coal specimens, the content of volatile matter and the number of active functional groups in the coal decrease, leading to a reduction in the oxidation trait of the coal [31,32]. Table 2 illustrates that with an increase in the metamorphic grade of the coal sample, both the decay rate of O<sub>2</sub> concentration and the volumetric O<sub>2</sub> depletion rate within the device decrease while the steady-state oxygen concentration increases.

**Figure 7.** Oxygen concentration versus time curve. DY: Dayan, JDL: Jiudaoling, DW: Duanwang.**Table 2.** Oxidation parameters of coal samples at different levels of metamorphism.

Coal sample	Coal variety	$\lambda c$ (min <sup>-1</sup> )	C <sub>b</sub> (%)	$\gamma$ (mol m <sup>-3</sup> min <sup>-1</sup> )
DY	Brown coal	1.47×10 <sup>-3</sup>	4.41	1.0856×10 <sup>-2</sup>
JDL	Long flame coal	1.16×10 <sup>-3</sup>	7.06	6.759×10 <sup>-3</sup>
DW	Meager coal	6.00×10 <sup>-4</sup>	18.24	1.0856×10 <sup>-4</sup>

DY: Dayan, JDL: Jiudaoling, DW: Duanwang.

Significant differences exist in the steady-state oxygen concentration among coal specimens exhibiting varying levels of metamorphic change. Therefore, dividing the spontaneous combustion “three zones” utilizing the oxidative traits of coal samples is critically significant. The key oxygen concentration for the suffocation zone (steady state) of JDL coal samples was determined to be 7.06%, providing a basis for simulation.

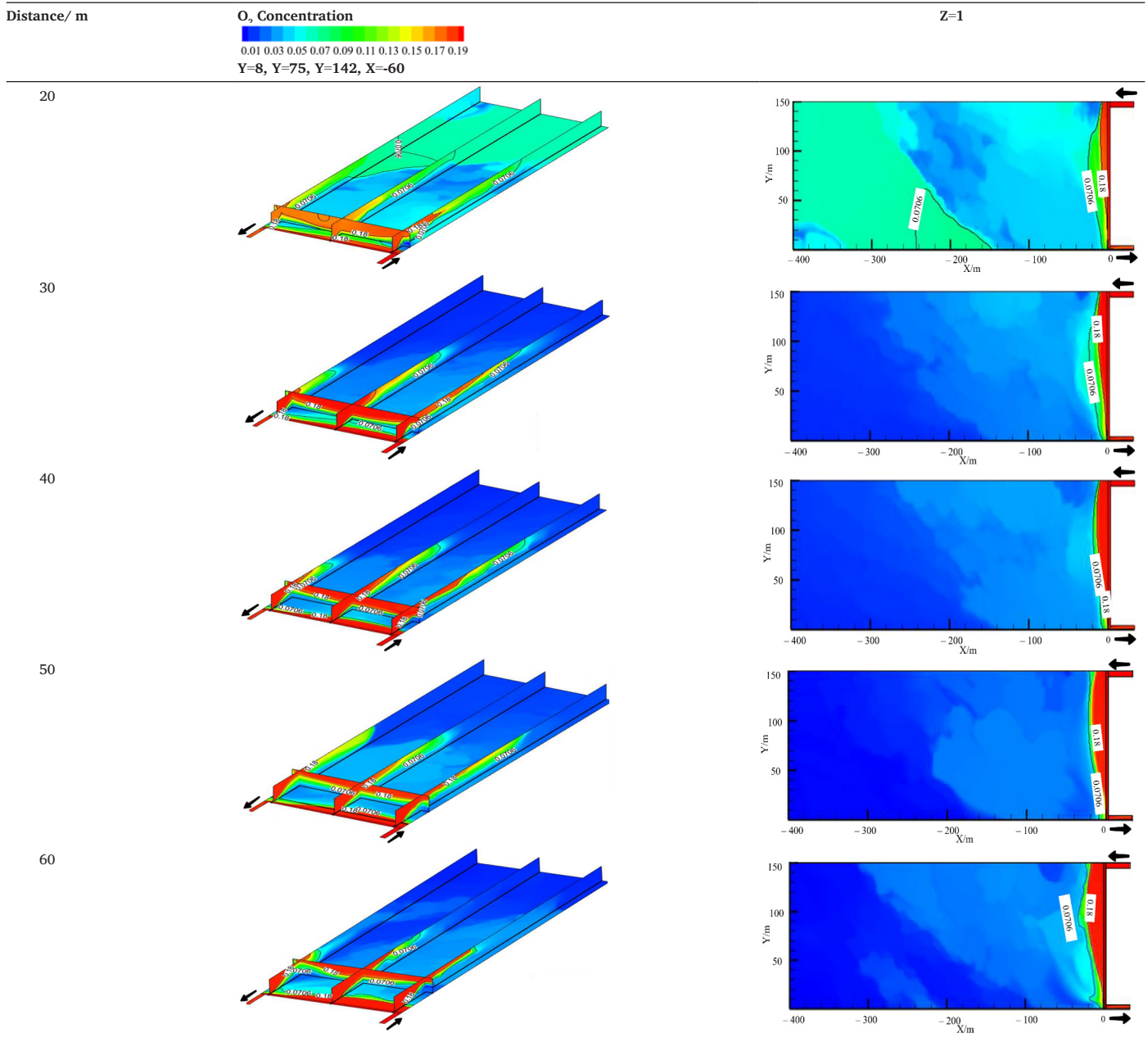
#### 3.2. CO<sub>2</sub> injection parameters

##### 3.2.1. Selection of CO<sub>2</sub> injection port location

To determine the optimal location for CO<sub>2</sub> injection, five injection ports were set on the side near the intake airway. Under the condition of a fixed CO<sub>2</sub> injection rate of 420 m<sup>3</sup>/h, simulations were conducted to determine the O<sub>2</sub> concentration distribution within the goaf for various injection port positions away from the working face. Since the relative molecular mass of CO<sub>2</sub> is greater than the average molecular mass of air, when CO<sub>2</sub> gas is injected into the goaf, it typically accumulates on the goaf floor due to the influence of gravity. This accumulation phenomenon affects the distribution of O<sub>2</sub> in the goaf, reducing its concentration through displacement effects and driving some CO<sub>2</sub> to move towards the top of the goaf. This results in a decrease in the interaction surface between oxygen and leftover coal on the floor of the goaf, consequently mitigating the oxidative processes of the leftover coal within the goaf and reducing the expanse of the oxidation zone. Table 3 illustrates the O<sub>2</sub> concentration distribution within the goaf across various CO<sub>2</sub> injection locations.

In contrast to the broadest extent of the oxidation zone within the goaf in the absence of CO<sub>2</sub> injection, the zone extent was reduced by 89.6% following CO<sub>2</sub> injection at the x = -20 location. However, this reduction rate is the lowest among all five injection port locations examined. The occurrence of this situation is mainly attributed to the intense leakage around the working face, which leads to rapid CO<sub>2</sub> gas flow back, affecting uniform coverage throughout the entire goaf. As the separation from the injection point to the working face grows, the effect gradually lessens. However, with greater distance from the injection

**Table 3.** O<sub>2</sub> concentration distribution in goaf at various CO<sub>2</sub> injection locations.



port to the working face, the airflow may not effectively deliver the CO<sub>2</sub> gas across the entire oxidation zone, resulting in a rebound of the zone's maximum breadth. Maximum extent of the oxidation zone initially decreases and then increases, consistent with the findings of Jiang *et al.* [33]. Figure 8 illustrates the variation in the largest span of the oxidation zone corresponding to shifts in the position of the gas injection port. It was calculated that when situating the injection port roughly 43 m away from the intake side of the working face, the maximum extent of the goaf's oxidation zone achieves its minimum extent.

**3.2.2. Determination of CO<sub>2</sub> injection rate**

Theoretically, increasing the CO<sub>2</sub> injection rate can more effectively displace O<sub>2</sub> in goaf, thereby narrowing the extent of the oxidation zone and curbing the CSC within the goaf. However, increases in injection rates, if unlimited, not only lead to rising costs but also may cause excessive CO<sub>2</sub> to backflow into the return airway, resulting in

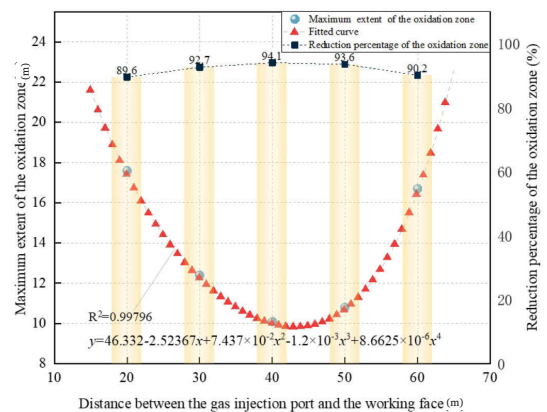
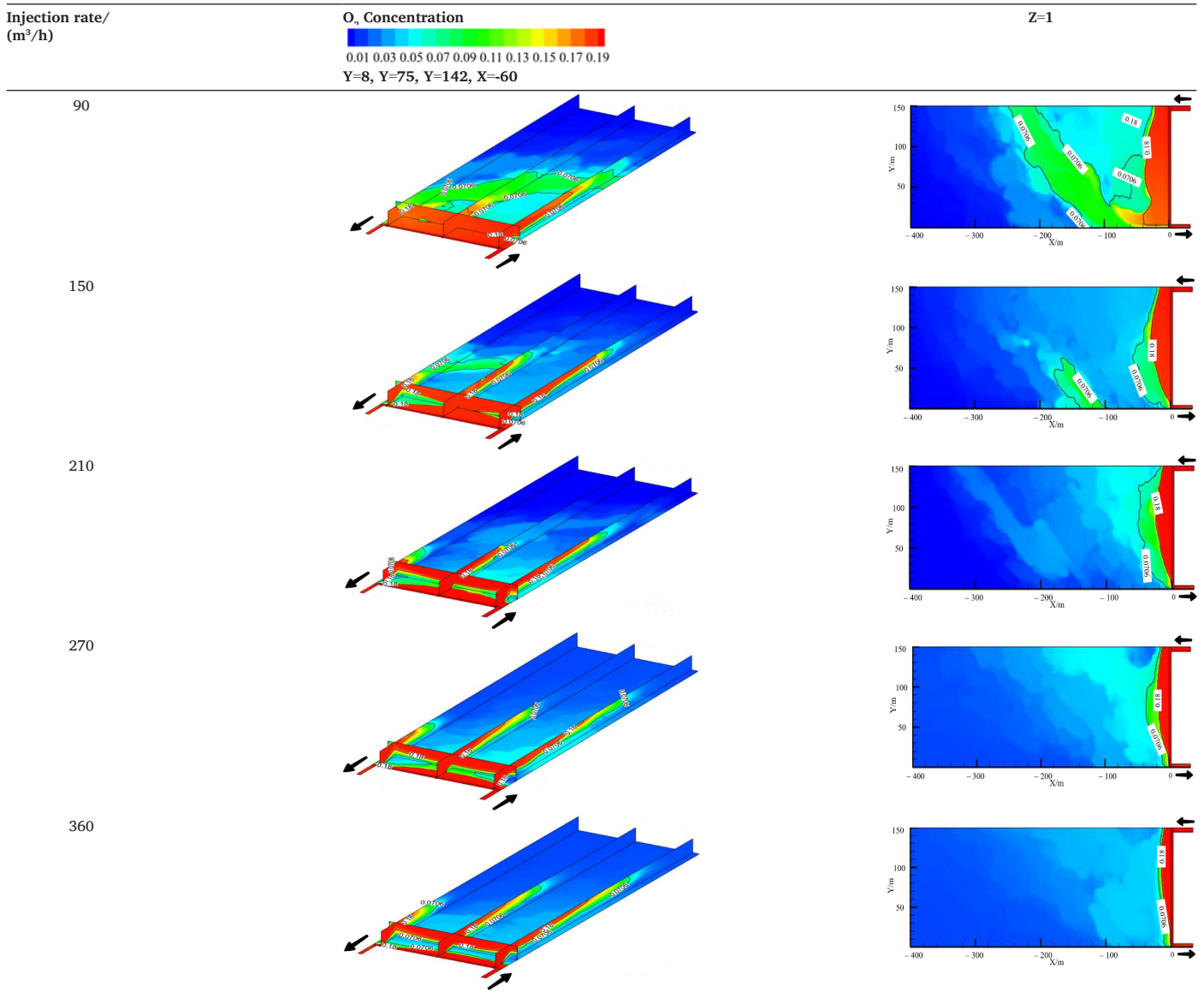


**Figure 8.** Variation of maximum oxidation zone extent with gas injection port position.

**Table 4.** Distribution of O<sub>2</sub> concentration in goaf under varying injection rates.



concentration exceedances. Therefore, it is crucial to determine a reasonable CO<sub>2</sub> injection rate. At an injection port distance of 43 m from the working face, simulations were conducted with injection rates of 90, 150, 210, 270, and 360 m<sup>3</sup>/h. The simulation results have been shown in Table 4. With the augmentation of the injection rate, there is a progressive reduction in the maximal breadth of the oxidation zone. Figure 9 illustrates the relationship between the CO<sub>2</sub> injection rate and the distribution of the O<sub>2</sub> in goaf.

The average advancement rate of the JDL E1S6 working face is 1.8 m/d, and the shortest spontaneous combustion period is 21 days.

The maximum allowable extent of the oxidation zone in goaf, as shown in Eq. (3).

$$L_m = v \cdot \tau \quad (3)$$

where  $L_m$  is the maximum allowable extent of the oxidation zone, m.  $v$  is the daily advance rate of the working face, m/d.  $\tau$  is the shortest spontaneous combustion period, d.

The maximum allowable extent of the oxidation zone in goaf was calculated to be 37.8 m, with the corresponding minimum CO<sub>2</sub> injection rate of 156.9 m<sup>3</sup>/h, which should be considered the optimal injection rate for CO<sub>2</sub> injection in goaf of JDL coal mine.

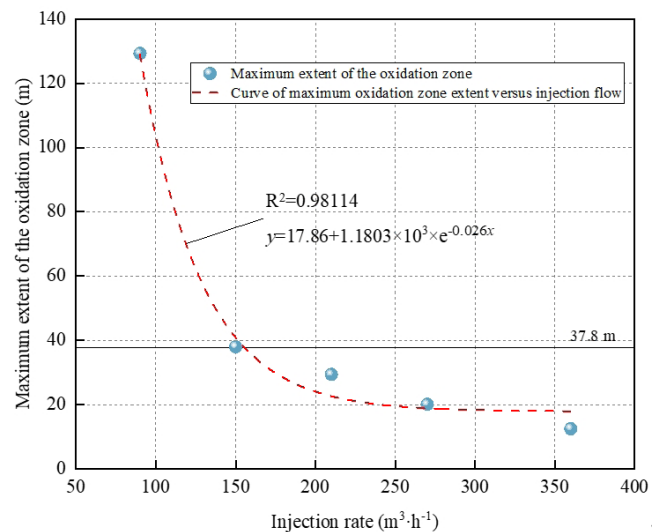


**Figure 9.** Variation of maximum oxidation zone extent with gas injection rate.

#### 4. Conclusions

In this paper, through sealed oxidation experiments, field measurements, and numerical simulations, the key oxygen concentration of the suffocation zone for JDL coal samples was determined. This critical oxygen concentration was then applied to the numerical simulation of CO<sub>2</sub> injection in the goaf of the JDL coal mine, identifying the optimal injection location and rate. The focused results can be summarized as follows:

A comparative analysis of the oxidation traits of coal samples from JDL, DY, and DW revealed that as the degree of coal metamorphism increases, the steady state oxygen concentration tends to rise, while the volume oxygen depletion rate and oxygen concentration decay rate correspondingly decrease. The correlation between the degree of coal sample metamorphism and the changes in oxygen concentration during the oxidation process was revealed.

Using numerical simulation methods, the extent of the oxidation zones on the intake and return sides of the goaf were obtained as 167 m and 98 m, respectively. The errors compared to the field measurements for the intake and return sides were 2.3% and 1.02%, respectively. As the distance between the injection port and the working face extends, the maximum width of the oxidation zone demonstrates a trend of initially narrowing before subsequently widening. The CO<sub>2</sub> injection rate within goaf is inversely related to the extent of the spontaneous combustion oxidation zone.

Considering the specific conditions of the JDL coal mine, the optimal injection location was determined to be on the intake side 43 m away from the working face, with an optimal injection rate of 156.9 m<sup>3</sup>/h. Future studies will delve more profoundly into the correlation between the properties of coal oxidation and the effectiveness of CO<sub>2</sub> inertization within the goaf.

#### CRedit authorship contribution statement

**Suoran Huang:** Investigation, Formal analysis, Writing-original draft, Writing-review & editing. **Zongxiang Li:** Software, Funding acquisition, Resources, Supervision. **Yu Liu:** Investigation, Conceptualization. **Ji Wu:** Formal analysis, Visualization, Formal analysis, Resources, Writing-review.

#### Declaration of competing interest

The authors declare that they have no known competing financial interests or personal relationships that could have appeared to influence the work reported in this paper.

#### Data availability

The datasets used and/or analysed during the current study available from the corresponding author on reasonable request.

#### Declaration of generative AI and AI-assisted technologies in the writing process

The authors confirm that there was no use of artificial intelligence (AI)-assisted technology for assisting in the writing or editing of the manuscript and no images were manipulated using AI.

#### Acknowledgment

This study was financially supported by National Natural Science Foundation of China (51774170).

#### References

- Zheng, Y., Li, S., Xue, S., Jiang, B., Ren, B., Zhao, Y., 2023. Study on the evolution characteristics of coal spontaneous combustion and gas coupling disaster region in goaf. *Fuel*, **349**, 128505. <https://doi.org/10.1016/j.fuel.2023.128505>
- Li, Z., Li, L., Si, J., Yang, X., 2024. New exploration on the goaf inerting with hidden fire source under CO<sub>2</sub> injection volume of adsorption compensation. *Case Studies in Thermal Engineering*, **62**, 105203. <https://doi.org/10.1016/j.csite.2024.105203>

- Ma, L., Zhang, P.-Y., Chen, X.-K., He, Y.-P., Wei, G.-M., Fan, J., 2024. Numerical investigation of coupling hazard zone of coal spontaneous combustion and gas in gob for high-gas mines. *Case Studies in Thermal Engineering*, **63**, 105341. <https://doi.org/10.1016/j.csite.2024.105341>
- Huang, X., Rein, G., 2014. Smouldering combustion of peat in wildfires: Inverse modelling of the drying and the thermal and oxidative decomposition kinetics. *Combustion and Flame*, **161**, 1633-1644. <https://doi.org/10.1016/j.combustflame.2013.12.013>
- Lu, X., Zhu, H., Wang, D., Hu, C., Zhao, H., Huo, Y., 2018. Flow characteristic investigation of inhibition foam used for fire extinguishment in the underground goaf. *Process Safety and Environmental Protection*, **116**, 159-168. <https://doi.org/10.1016/j.psep.2018.02.005>
- Li, Z., Huang, S., Li, L., Si, J., Wu, J., 2024. Study on CO dispersion characteristics and isolation door control technology of refuge chamber in coal mine. *Scientific Reports*, **14**, 21553. <https://doi.org/10.1038/s41598-024-72188-3>
- Li, Z., Wang, Y., Li, L., 2015. 3D simulation of disaster process in mine ventilation system during fire period. *Journal of China Coal Society*, **40**, 115-121. <https://doi.org/10.16265/j.cnki.issn1003-3033.2015.08.007>
- Song, Z., Kuenzer, C., 2014. Coal fires in China over the last decade: A comprehensive review. *International Journal of Coal Geology*, **133**, 72-99. <https://doi.org/10.1016/j.coal.2014.09.004>
- Pan, R., Cheng, Y., Yu, M., Lu, C., Yang, K., 2013. New technological partition for "three zones" spontaneous coal combustion in goaf. *International Journal of Mining Science and Technology*, **23**, 489-493. <https://doi.org/10.1016/j.ijmst.2013.07.005>
- Jia, X., Qi, Q., Zhao, Y., Zhou, X., Dong, Z., 2021. Determination of the spontaneous combustion hazardous zone and analysis of influencing factors in bedding boreholes of a deep coal seam. *ACS omega*, **6**, 8418-8429. <https://doi.org/10.1021/acsomega.1c00139>
- Hao, Y., Xie, T., 2021. Oxidation behavior and kinetics parameters of a lean coal at low temperature based on different oxygen concentrations. *Minerals*, **11**, 511. <https://doi.org/10.3390/min11050511>
- Xu, J., Deng, J., Wen, H., 1998. Analysis of possible ignition area in goaf of coal face. *Journal of Xi'an University of Science and Technology*, **1**, 14-23.
- Xie, J., Xue, S., 2011. Study on division index and method of three spontaneous combustion zones in goaf of fully mechanized top coal caving mining face. *Coal Science And Technology*, **39**, 65-8. <https://doi.org/10.13199/j.cst.2011.01.71.xiej.022>
- Song, W., Yang, S., Xu, Q., 2012. Division of spontaneous combustion "three-zone" in high-gas goaf based on oxygen concentration. *Journal of Mining & Safety Engineering*, **29**, 271-6.
- Wei, D., Du, C., Lei, B., Lin, Y., 2020. Prediction and prevention of spontaneous combustion of coal from goafs in workplace: A case study. *Case Studies in Thermal Engineering*, **21**, 100668. <https://doi.org/10.1016/j.csite.2020.100668>
- Gui, X., Xue, H., Zhan, X., Hu, Z., Song, X., 2022. Measurement and numerical simulation of coal spontaneous combustion in goaf under y-type ventilation mode. *ACS omega*, **7**, 9406-9421. <https://doi.org/10.1021/acsomega.1c06703>
- Zhuo, H., Qin, B., Qin, Q., Su, Z., 2019. Modeling and simulation of coal spontaneous combustion in a gob of shallow buried coal seams. *Process Safety and Environmental Protection*, **131**, 246-254. <https://doi.org/10.1016/j.psep.2019.09.011>
- Zong-xiang, L., Yu, L., Bang-da, W., Hui-bo, Z., Jin-zhang, J., Xian-kui, C., 2017. Critical oxygen volume fraction of smothering quenched zone based on closed oxygen consumption experiment. *Journal of China Coal Society*, **42**, 1776-1781. <https://doi.org/10.13225/j.cnki.jccs.2016.1386>
- Shao, H., Jiang, S., Wu, Z., Zhang, W.-Q., 2013. Numerical simulation on fire prevention by infusing carbon dioxide into goaf. *Journal of Mining & Safety Engineering*, **30**, 154-8.
- Ding, C., Li, Z., Wang, J., Lu, B., Gao, D., 2023. Effects of inert gas CO<sub>2</sub>/N<sub>2</sub> injection on coal low-temperature oxidation characteristic: Experiments and simulations. *Arabian Journal of Chemistry*, **16**, 104510. <https://doi.org/10.1016/j.arabj.2022.104510>
- Yang, S., Zhou, B., Wang, C., 2021. Investigation on coal spontaneous combustion in the gob of Y type ventilation caving face: A case study. *Process Safety and Environmental Protection*, **148**, 590-603. <https://doi.org/10.1016/j.psep.2020.11.024>
- Qiao, M., Ren, T., Roberts, J., Yang, X., Li, Z., Wu, J., 2022. New insight into proactive goaf inertisation for spontaneous combustion management and control. *Process Safety and Environmental Protection*, **161**, 739-757. <https://doi.org/10.1016/j.psep.2022.03.074>
- Hao Z., Wang J., Huang G., He F., 2015. Study on inject position of low temperature CO<sub>2</sub> in gob based on coupling effect of inerting cooling. *Journal of Safety Science and Technology*, **11**, 17-23.
- Huang, G., Wang, J., Dai, F., Deng, C., 2020. Targeted inertization with flue gas injection in fully mechanized caving gob for residual coal spontaneous combustion prevention with CFD modeling. *Energy Science & Engineering*, **8**, 3961-3979. <https://doi.org/10.1002/ese3.789>
- Qiao, M., Ren, T., Roberts, J., Liu, H., Yang, X., Tan, L., Wu, J., 2022. Improved computational fluid dynamics modelling of coal spontaneous combustion control and gas management. *Fuel*, **324**, 124456. <https://doi.org/10.1016/j.fuel.2022.124456>
- Lu, B., Zhang, X., Qiao, L., Ding, C., Fan, N., Huang, G., 2024. Experimental study on the effect of slow reaction process of the latent period on coal spontaneous combustion. *Energy*, **302**, 131927. <https://doi.org/10.1016/j.energy.2024.131927>
- Li, Z., Zhang, M., Yang, Z., Yu, L., Cong, D., Ge, H., 2023. Effect of fault structure on the structure and oxidative spontaneous combustion characteristics of coal. *Journal of China Coal Society*, **48**, 1246-1254. <https://doi.org/10.13225/j.cnki.jccs.2021.1798>
- Hu, D., Li, Z., Liu, Y., Ding, C., Miao, C., Wang, H., 2024. Effects of stratified mining on the low-temperature oxidation and physicochemical properties of lower coal layers. *Arabian Journal of Chemistry*, **17**, 105476. <https://doi.org/10.1016/j.arabj.2023.105476>

29. Li, Z., Li, Y., Hu, D., 2023. Study on the risk assessment of coal spontaneous combustion in U+L type ventilation stopes with roof cutting gob-side entry retaining. *Journal of Natural Disasters*, **32**, 240-246.
30. Li, Z., Gu, R., Zhang, X., Bi, Q., Wen, Y., 2014. Simulation of gas migration in 3D goaf based on RNG k- $\epsilon$  turbulence model. *Journal of China Coal Society*, **39**, 880-5. <https://doi.org/10.13225/j.cnki.jccs.2013.0640>
31. Deng, J., Hu, P., Bai, Z.-J., Wang, C.-P., Kang, F.-R., Liu, L., 2022. Dynamic behaviours on oxidation heat release of key active groups for coal with different degrees of metamorphism. *Fuel*, **320**, 123967. <https://doi.org/10.1016/j.fuel.2022.123967>
32. Li, Z., Zhang M., Liu Y., Yang Z., Miao C., Wang H., Xu H., 2023. Relational analysis of coal oxidation exothermic characteristics and affecting factors. *Journal of Safety and Environment*, **23**, 49-56. <https://doi.org/10.13637/j.issn.1009-6094.2021.1581>
33. Jiang, K., Wang, Y., Ren, G., Xiangdong, Y., Kuibin, W., 2021. Study on the optimization simulation and application of technical parameters of CO<sub>2</sub> injection for fire prevention in goaf in 8059 working face of Yaoqiao Coal Mine. *Mining Safety & Environmental Protection*, **48**, 74-84. <https://doi.org/10.19835/j.issn.1008-4495.2021.03.014>